ORGANIC LETTERS

2007
Vol. 9, No. 5
845−848

# Biosynthetic Convergence of Salinosporamides A and B in the Marine Actinomycete *Salinispora tropica*

**Laura L. Beer[†] and Bradley S. Moore*[,†,‡]**

*College of Pharmacy, University of Arizona, Tucson, Arizona 85721, and Scripps Institution of Oceanography and the Skaggs School of Pharmacy and Pharmaceutical Sciences, University of California at San Diego, La Jolla, California 92093*

*bsmoore@ucsd.edu*

**Received December 21, 2006**

## ABSTRACT

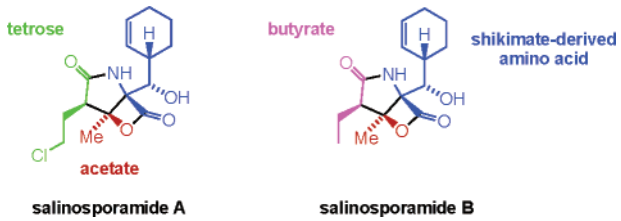


**Feeding experiments with stable isotopes established that the potent 20S-proteasome inhibitors salinosporamide A and B are biosynthesized in the marine bacterium *Salinispora tropica* from three biosynthetic building blocks, namely, acetate, β-hydroxy-2′-cyclohexenylalanine, and either butyrate or a tetrose-derived chlorinated molecule. The unexpected observation that the chlorinated four-carbon residue in salinosporamide A is derived from a different metabolic origin than the non-chlorinated four-carbon unit in salinosporamide B is suggestive of a convergent biosynthesis to these two anticancer natural products.**

Salinosporamide A is a potent anticancer agent that recently entered phase I human clinical trials for the treatment of multiple myeloma only 3 years after its discovery.[1,2] This novel marine natural product is produced by the recently described obligate marine bacterium *Salinispora tropica*[3] and belongs to a family of compounds possessing a densely functionalized γ-lactam-β-lactone bicycle.[4] This bicyclic ring structure has been reported once before in *clasto*-lactacystin-β-lactone (also called omuralide), a transformation product of lactacystin produced by the terrestrial actinomycete *Streptomyces lactacystinaeus*.[5] It is the unique functionality of salinosporamide A, however, that is responsible for its irreversible binding to the 20S-proteasome[6] rendering it ∼35 times more potent than omuralide in proteasome inhibition assays.[1] On the basis of the novel structure and potent activity of salinosporamide A, we set out to elucidate its biosynthesis through labeling studies with $^{13}$C-labeled intermediates in *S. tropica* CNB-476. The feeding experiments described herein not only established the biosynthetic building blocks of salinosporamides A (**1**) and B (**2**) but also revealed that their subtle structural difference involving the halogen atom results from the incorporation of alternate 4-carbon precursors indicative of promiscuous biosynthetic enzymes (Figure 1).

On the basis of the structure of salinosporamide A (**1**) and its deschloro analogue salinosporamide B (**2**) (Figure 1), we

[†] University of Arizona.
[‡] University of California at San Diego.

(1) Feling, R. H.; Buchanan, G. O.; Mincer, T. J.; Kauffman, C. A.; Jensen, P. R.; Fenical, W. *Angew. Chem., Int. Ed.* **2003**, *115*, 369−371.
(2) Chauhan, D.; Catley, L.; Li, G. L.; Podar, K.; Hideshima, T.; Velankar, M.; Mitsiades, C.; Mitsiades, N.; Yasui, H.; Letai, A.; Ovaa, H.; Berkers, C.; Nicholson, B.; Chao, T. H.; Neuteboom, S. T. C.; Richardson, P.; Palladino, M. A.; Anderson, K. C. *Cancer Cell* **2005,** *8*, 407−419.
(3) Maldonado, L. A.; Fenical, W.; Jensen, P. R.; Kauffman, C. A.; Mincer, T. J.; Ward, A. C.; Bull, A. T.; Goodfellow, M. *Int. J. System Evol. Microbiol.* **2005**, *55*, 1759−1766.
(4) Williams, P. G.; Buchanan, G. O.; Feling, R. H.; Kauffman, C. A.; Jensen, P. R.; Fenical, W. *J. Org. Chem.* **2005**, *70*, 6196−6203. Macherla, V. R.; Mitchell, S. S.; Manam, R. R.; Reed, K. A.; Fenical, W.; Neuteboom, S. T. C.; Lam, K. S.; Palladino, M. A.; Potts, B. C. M. *J. Med. Chem.* **2005**, *48*, 3684−3687.
(5) Corey, E. J.; Li, W. D. Z. *Chem. Pharm. Bull.* **1999**, *47*, 1−10.
(6) Groll, M.; Huber, R.; Potts, B. C. *J. Am. Chem. Soc.* **2006**, *128*, 5136−5141.

10.1021/ol063102o CCC: $37.00 
**Published on Web 02/03/2007**

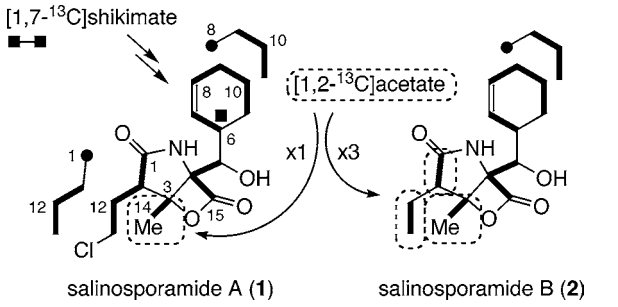


**Figure 1.** Origin of carbons in salinosporamides A (**1**) and B (**2**) from glucose (bold lines and circles), acetate (dashed boxes), and shikimate (square). $^{13}$C-isotopes from [U-$^{13}C_6$]glucose labeled the four-carbon fragments comprising carbons 1/2/12/13 of **1** and 8/9/10/11 of **1** and **2** in two patterns, both contiguously, as directly shown in the structures, and disjointed with single enrichment at C-1 in **1** and at C-8 in **1** and **2** as shown in the structural fragments.

hypothesized that **2** was a biosynthetic precursor of **1** and that halogenation of the unactivated C-13 methyl group might be catalyzed by a non-heme iron halogenase.[7] We anticipated that the carbons in **1** and **2** would be derived from three precursors, namely, acetate, butyrate, and a novel non-proteinogenic amino acid derived from phenylalanine. To our surprise, only one intact acetate unit was incorporated into **1** at C-3/C-14 ($J_{3,14}$ = 43 Hz) (Table 1).[8] Absolutely no label from [1,2-$^{13}C_2$]acetate was evident by $^{13}$C NMR spectroscopy in the four-carbon unit comprising C-1/C-2/C-12/C-13. This observation was corroborated with a subsequent incorporation experiment with [1-$^{13}$C]butyrate, which only labeled **1** at C-3 at 2.2% after $\beta$-oxidation to [1-$^{13}$C]-acetate.

To provide insight into the nature of the chlorinated four-carbon unit in **1** as well as the remaining cyclohexenyl unit, we next administered the general precursor [U-$^{13}C_6$]glucose to *S. tropica* CNB-476. This experiment resulted in the enrichment of all carbon atoms in **1** with discrete $^{13}$C-labeled intermediates through glycolysis and the Krebs cycle (Table 1). Analysis of the 1D $^{13}$C NMR spectrum from [U-$^{13}C_6$]-glucose-enriched **1** agreed with the results from the [1,2-$^{13}C_2$]acetate experiment as anticipated (Figure 1). Inspection

**Table 1.** $^{13}$C NMR Data of Salinosporamide A (**1**) and Incorporation Percentages of Labeled Precursors

| | | incorporation % | | | $J_{CC}$ (Hz) | |
|---|---|---|---|---|---|---|
| carbon | $\delta_c$, ppm[a] | [1-$^{13}C_1$] butyrate[b,c] | [1,3-$^{13}C_2$] glycerol[b,d] | [1,7-$^{13}C_2$] shikimate[b,c] | [1,2-$^{13}C_2$] acetate | [U-$^{13}C_6$] glucose |
| 1 | 177.4 | – | – | – | – | s[e], 47, 2 |
| 2 | 46.7 | – | 1.8 | – | – | 47, 36 |
| 3 | 86.8 | 2.2 | – | – | 43 | 43 |
| 4 | 80.8 | – | – | – | – | 47, 44 |
| 5 | 71.5 | – | 1.4 | – | – | 44, 3 |
| 6 | 39.8 | – | – | 1.2 | – | 42 |
| 7 | 129.6 | – | 1.5 | – | – | 42 |
| 8 | 129.2 | – | 1.3 | – | – | s[e], 39 |
| 9 | 25.9 | – | 1.5 | – | – | 36, 34 |
| 10 | 22.2 | – | – | – | – | 33[f] |
| 11 | 27.0 | – | 1.5 | – | – | 33 |
| 12 | 29.5 | – | – | – | – | 36[f] |
| 13 | 43.8 | – | 1.8 | – | – | 36 |
| 14 | 20.5 | – | 1.6 | – | 43 | 43 |
| 15 | 169.9 | – | – | – | – | 47, 3 |

[a] Referenced to $d_5$-pyridine. [b] % incorporation = ($A$ − $B$)/$B$, where $A$ = intensity of enriched carbon and B = intensity of the natural abundance carbon. [c] Incorporation relative to the natural abundance carbon at 177.4 ppm (C-1). [d] Incorporation relative to the natural abundance carbon at 22.2 ppm (C-10). [e] s = enriched singlet. [f] This signal represents a triplet.

of the four-carbon unit comprising C-1/C-2/C-12/C-13 in **1** revealed two overlapping $^{13}$C-labeled spin systems indicative of separate metabolic origins for these carbon atoms. Both labeled species were evident at C-2, which consisted of a doublet ($J_{2,12}$ = 36 Hz) and a doublet of doublets ($J_{1,2}$ = 47, $J_{2,12}$ = 36 Hz) in a 3:1 ratio flanking the natural abundance singlet at 46.7 ppm. The 36 Hz triplet at C-12 extended the intact $^{13}$C-spin system to the C-13 chloromethyl group. Further analysis of the $^{13}$C NMR signals in this contiguous four-carbon fragment confirmed the incorporation of intact and fragmented four-carbon units in a 1:3 ratio, respectively, in which the fragmented spin system is derived from single enrichment at C-1 and an enriched three-carbon unit at C-2/C-12/C-13 (Figure 1).

This same labeling pattern involving two overlapping $^{13}$C-labeled spin systems was also evident in another four-carbon unit spanning C-8 through C-11 in the cyclohexenyl moiety ($J_{8,9}$ = 36, $J_{9,10}$ = 34, $J_{10,11}$ = 33 Hz) in which C-8 like C-1 was both singly and doubly enriched (Figure 1). The remainder of the cyclohexene ring was labeled with an intact two-carbon unit at C-6/C-7 ($J_{6,7}$ = 42 Hz), whereas C-4/C-5/C-15 was derived from a three-carbon unit ($J_{4,5}$ = 44, $J_{4,15}$ = 36, and $^2J_{5,15}$ = 3 Hz). Taken together, this labeling pattern in the amino acid derived moiety in **1** is reminiscent of that in phenylalanine biosynthesis[9] with one key difference. The asymmetrical labeling of the six-membered ring implied that the two sides of the ring must remain distinct throughout the biosynthetic process, which would not be the case if derived from phenylalanine or another aromatic intermediate. This observation suggested a novel shunt in the aromatic amino acid biosynthetic pathway prior to the conversion of

(7) Vaillancourt, F. H.; Yeh, E.; Vosburg, D. A.; Garneau-Tsodikova, S.; Walsh, C. T. *Chem. Rev.* **2006**, *106*, 3364−3378.

(8) *S. tropica* CNB-476 was cultured in seawater-based media (28 g of Instant Ocean, 4 g of yeast extract, 10 g of soluble starch, 1 g of $CaCO_3$, 2 g of peptone, 5 mL of $Fe_2SO_4$ (8%), 5 mL of KBr (20%), and 10 mL of Tris (pH 7) in 1 L of $H_2O$) and shaken at 30 °C for 5−7 days. Labeled precursors were added to 200 mL cultures with Amberlite XAD-7 resin after 24−36 h of growth in the following concentrations: [1,2-$^{13}C_2$]acetate (50 mg/L), [U-$^{13}C_6$]glucose (50 mg/L), [1,3-$^{13}C_2$]glycerol (100 mg/L), [1-$^{13}C_1$]butyrate (125 mg/L), [1,7-$^{13}C_2$]shikimic acid (125 mg/L), and [7-$^{13}C_1$]phenylalanine (125 mg/L). [1,7-$^{13}C_2$]Shikimic acid was generously provided by Professor Heinz G. Floss (University of Washington), whereas all other labeled compounds were purchased from Cambridge Isotope Laboratories. The resin was isolated from cultures and extracted with ~500 mL of acetone. Dried crude extracts were subjected to reversed-phase HPLC (YMC 20 × 250 mm, 10 $\mu$m) employing a gradient of 30% MeCN to 70% MeCN over 20 min with a flow rate of 9.5 mL/min and UV monitoring at 225 nm to yield salinosporamide A (70−100 mg/L). Salinosporamide B (10−20 mg/L) was alternatively purified by normal-phase isocratic silica gel flash column chromatography (Merck, grade 9385, 230−400 mesh).

(9) Phenylalanine is biosynthesized by a well-established pathway in which glucose is converted via erythrose 4-phosphate and 2 equiv of phosphoenolpyruvate to shikimate and chorismate. Haslam, E. *The Shikimate Pathway*; Halsted Press: New York, 1974.

prephenate to phenylpyruvate (via prephenate dehydratase) in which the chirality of the cyclohexyl ring is lost during aromatization as proposed in Scheme 1.[10] To evaluate this

**Scheme 1.** Proposed Biosynthesis of the Nonproteinogenic Amino Acid $\beta$-Hydroxycyclohex-2′-enylalanine (**3**) (R = H or S−PCP) via a Shunt in the Phenylalanine Biosynthetic Pathway

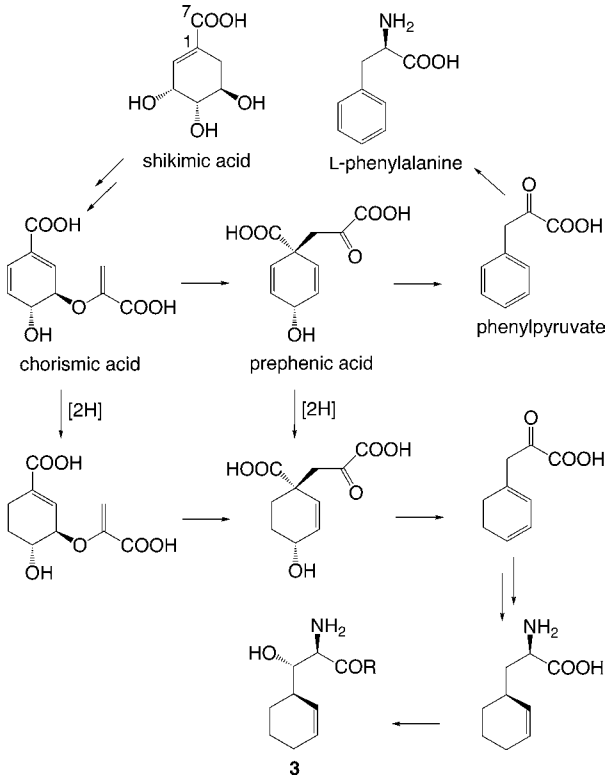


hypothesis, we tested the pathway intermediacy of shikimic acid and phenylalanine. The specific incorporation of a single $^{13}C$ atom from dually labeled [1,7-$^{13}C_2$]shikimic acid at C-6 (1.2%) in **1** (Figure 1) not only verified the intermediacy of shikimate but also established that the C-7 carboxyl group of shikimate is lost in the transformation. As expected from the [U-$^{13}C_6$]glucose experiment,[10] [1-$^{13}C$]phenylalanine was not assimilated into the natural product. These findings support a shunt pathway toward the biosynthesis of the novel non-proteinogenic amino acid residue $\beta$-hydroxycyclohex-2′-enylalanine (**3**) (Scheme 1).

The dual labeling pattern of the four-carbon fragment in the shikimate-derived cyclohexenyl moiety, which originates from erythrose 4-phosphate, is consistent with an active glycolytic pathway in *S. tropica*. Hence, the observation that the $\gamma$-lactam four-carbon unit in **1** has the identical glucose labeling pattern was suggestive of a tetrose origin of the chlorinated fragment. This observation was corroborated through a separate experiment in which the triose [1,3-$^{13}C_2$]-glycerol[11] was administered and resulted in single enrichment at C-2 and C-13 (Table 1). The $^{13}C$-incorporation observed in the four-carbon unit was contrary to our original biosynthetic hypothesis for **1** in which we proposed that **2** was the biosynthetic precursor of **1** and that the four-carbon unit arose from butyrate. Given that the reported pathways for butyryl-CoA biosynthesis in actinomycetes utilize acetate and/or valine metabolic building blocks,[12] the observed $^{13}C-^{13}C$ coupling pattern from the acetate and glucose experiments discounted the intermediacy of butyryl-CoA in the biosynthesis of **1**.

To further explore the unusual four-carbon building block in **1**, we evaluated the intermediacy of the isoleucine catabolite 2-methylbutyrate, which we hypothesized could parallel valine-derived methylmalonyl-semialdehyde in lactacystin biosynthesis,[13] in which oxidation could directly provide ethylmalonyl-CoA. However, there was no incorporation of a label from 2-methyl[2-$^{13}C_1$]butyrate in **1** upon administration to *S. tropica*. These experiments systematically eliminated pathways involving branched-chain amino acid metabolism or butyrate biosynthesis.

We next turned our attention to salinosporamide B (**2**) to explore its biosynthetic origins. As originally anticipated, $^{13}C$ NMR analysis of [1,2-$^{13}C_2$]acetate-enriched **2** revealed the intact incorporation of three acetate units at not only C-3/C-14 ($J_{13,14}$ = 42 Hz) like in **1** but also C-1/C-2 ($J_{1,2}$ = 46 Hz) and C-12/C-13 ($J_{12,13}$ = 35 Hz), which is consistent with the intermediacy of butyrate. The incorporation of a $^{13}C$-label from [U-$^{13}C_6$]glucose into **2** further showed that the four-carbon units in **1** and **2** are assembled via distinct precursors (Figure 1).

Whereas **1** and **2** share the biosynthetic precursors acetate and presumed $\beta$-hydroxycyclohex-2′-enylalanine (**3**), they differ in the origin of the four-carbon building block that gives rise to their structural difference involving the halogen atom. We propose a hybrid polyketide synthase−nonribosomal peptide synthetase (PKS−NRPS) pathway for the biosynthesis of **2** in which acetyl-CoA- and butyrate-derived ethylmalonyl-CoA condense to yield the $\beta$-ketothioester **4**, which then reacts with **3** to generate the linear precursor **5** (Scheme 2).

Formation of the bicyclic ring system likely occurs in a stepwise manner from **5** and is initiated with the abstraction of the α-hydrogen of the amino acid residue to form the $\gamma$-lactam. Attack of the ensuing oxyanion on the thioester carbonyl would complete the biosynthesis and liberate the product **2** from the peptidyl carrier protein (PCP). By analogy, the biosynthesis of **1** is proposed to involve a related pathway in which the butyrate unit of **2** is replaced with the unprecedented PKS extender unit chlorobutyrate, which would originate from a sugar precursor.

In contrast, the fused $\gamma$-lactam-$\beta$-lactone ring system of omuralide is derived from the chemical transformation of

(10) If the cyclohexenyl unit was indeed derived from phenylpyruvate or a related metabolite, the [U-$^{13}C_6$]glucose enrichment would provide two equally labeled species, one of which is shown in Figure 1 and the second involving two- and four-carbon spin systems at C-6/C-11 and C-7/C-8/C-9/C-10, respectively, which is not the case.

(11) Glycerol can enter the glycolytic pathway via dihydroxyacetone phosphate.

(12) Liu, H. B.; Reynolds, K. A. *Metab. Eng.* **2001**, *3*, 40−48.

(13) Nakagawa, A.; Takahashi, S.; Uchida, K.; Matsuzaki, K.; Omura, S.; Nakamura, A.; Kurihara, N.; Nakamatsu, T.; Miyake, Y.; Take, K.; Kainosho, M. *Tetrahedron Lett.* **1994**, *35*, 5009−5012. Takahashi, S.; Uchida, K.; Nakagawa, A. *J. Antibiot.* **1995**, *48*, 1015−1020.

**Scheme 2.** Proposed Biosynthesis of the Hybrid Polyketide-Peptides **1** and **2** Involving a Novel Off-Loading Reaction

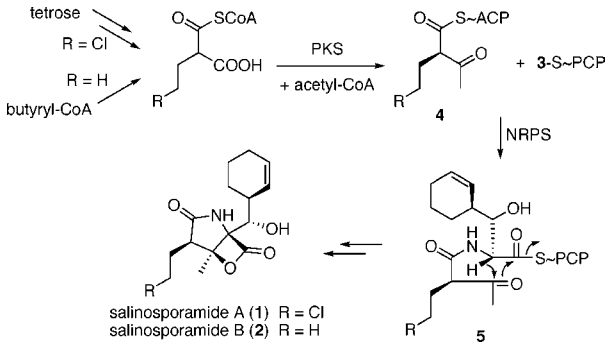


the streptomycete natural product lactacystin involving the loss of *N*-acetylcysteine and concomitant formation of the $\beta$-lactone unit.[5] Feeding experiments with general precursors established that the lactacystin $\gamma$-lactam moiety is rather assembled via a condensation between valine-derived methylmalonic semialdehyde and the α-carbon of leucine followed by an intramolecular condensation.[13] The biosynthesis of the salinosporamides differs from that of lactacystin and thus omuralide, as all three side chains are derived from distinct biosynthetic building blocks, which originate via an unprecedented PKS−NRPS pathway. The engineered biosynthesis of new salinosporamide derivatives utilizing unnatural biosynthetic building blocks for structure−activity relationship studies will be reported elsewhere.

**Acknowledgment.** We thank W. Fenical and P. R. Jensen (Scripps Institution of Oceanography) and R. Lam (Nereus Pharmaceuticals, Inc.) for the strain *Salinispora tropica* CNB-476, salinosporamide standards, and helpful discussions and J. Kalaitzis, N. Jacobsen, and J. Dai (University of Arizona) for assistance with NMR experiments. This work was supported by grants from Washington Sea Grant (R/B-47) and Nereus Pharmaceuticals, Inc. to B.S.M. and a National Sea Grant−Industry graduate fellowship to L.L.B.

**Supporting Information Available:** NMR spectra of $^{13}$C-labeled salinosporamide A and B. This material is available free of charge via the Internet at http://pubs.acs.org.

OL063102O